ORNL/TM-2023/3046

Mechanical Properties of Zircaloy Cladding Tubes and Contributions to M.E.T.A. Mechanical Property Database

Ben Garrison
Caleb Massey
Weiju Ren
Maxim Gussev
Tim Graening
Robert Sitterson
Nathan Capps
Kory Linton

August 2023

M3FT-23OR020204043

OAK RIDGE National Laboratory

ORNL IS MANAGED BY UT-BATTELLE LLC FOR THE US DEPARTMENT OF ENERGY

DOCUMENT AVAILABILITY

Reports produced after January 1, 1996, are generally available free via OSTI.GOV.

Website www.osti.gov

Reports produced before January 1, 1996, may be purchased by members of the public from the following source:

National Technical Information Service
5285 Port Royal Road
Springfield, VA 22161
Telephone 703-605-6000 (1-800-553-6847)
TDD 703-487-4639
Fax 703-605-6900
E-mail info@ntis.gov
Website http://classic.ntis.gov/

Reports are available to US Department of Energy (DOE) employees, DOE contractors, Energy Technology Data Exchange representatives, and International Nuclear Information System representatives from the following source:

Office of Scientific and Technical Information
PO Box 62
Oak Ridge, TN 37831
Telephone 865-576-8401
Fax 865-576-5728
E-mail reports@osti.gov
Website https://www.osti.gov/

ORNL/TM-2023/3046

Nuclear Energy Fuel Cycle Division

MECHANICAL PROPERTIES OF ZIRCALOY CLADDING TUBES AND CONTRIBUTIONS TO M.E.T.A. MECHANICAL PROPERTY DATABASE

Ben Garrison
Caleb Massey
Weiju Ren
Maxim Gussev
Tim Graening
Robert Sitterson
Nathan Capps
Kory Linton

August 2023

DOE Milestone #M3FT-23OR020204043

Prepared by
OAK RIDGE NATIONAL LABORATORY
Oak Ridge, TN 37831
managed by
UT-BATTELLE LLC
for the
US DEPARTMENT OF ENERGY
under contract DE-AC05-00OR22725

CONTENTS

LIST OF FIGURES iv
LIST OF TABLES v
ABSTRACT 2
1. INTRODUCTION 2
    1.1 AXIAL TENSION AND RING TENSION MECHANICAL PROPERTY CORRELATIONS 2
    1.2 AXIAL TENSION AND RING TENSION MECHANICAL PROPERTY DATABASE 3
2. MATERIALS AND TESTING 3
3. RESULTS AND DISCUSSION 5
    3.1 ZIRCALOY-4 PLATE TESTING 5
    3.2 ZIRCALOY-4 AND COATING IMPACT ON MECHANICAL PROPERTIES 9
4. MATERIALS DATABASE 12
5. CONCLUSIONS 14
6. REFERENCES 15

LIST OF FIGURES

Figure 1. Specimen drawings of a) the ATT specimen and b) RTT specimen used in this work with c) a schematic showing the load configuration of the fixture used to load RTT specimens. 4
Figure 2. Machining schema for the ATT, RTT, and SSJ3 specimens that were manufactured out of Zircaloy-4 plate 4
Figure 3. Mechanical test results of the fully recrystallized Zircaloy-4 plate. 5
Figure 4. Engineering mechanical properties obtained for the fully recrystallized Zircaloy-4 plate showing that trends among the tensile geometries and cutting directions are maintained. 7
Figure 5. Correlation plots comparing the a) stress-based and b) strain-based engineering properties obtained from ATT specimens vs. those obtained from SSJ3 specimens tested under the same conditions. 7
Figure 6. Engineering property correlations between RTT specimens and ATT specimens tested at the same conditions. 9
Figure 7. Mechanical test results a) at RT and b) at 300ºC for ATT specimens machined from AFC Zircaloy-4 tubing and coated tubing. 10
Figure 8. Mechanical tests with ATT specimens at RT showing the difference between the mechanical response of EDMed specimens vs. those end-milled on a CNC. 11
Figure 9. Mechanical test results a) at RT and b) at 300°C for RTT specimens machined from AFC Zircaloy-4 tubing and coated tubing. 12
Figure 10. Image of the database interface showing how various specimen and material inputs can be tracked and accessed. 13
Figure 11. Example image of a table output from the database showing the engineering properties that can be accessed as well as functional data such as the stress strain curves (not depicted) 14

LIST OF TABLES

Table 1. Engineering mechanical properties obtained from Zircaloy-4 plate. 6
Table 2. Mechanical properties obtained from ATT tests machined from AR and coated AFC-Zircaloy-4 tubing. 10
Table 3. Engineering mechanical properties obtained from RTT specimens machined from AFC Zircaloy-4 tubing tested at RT and 300°C. 12

ACKNOWLEDGMENTS

This research is supported by the Advanced Fuel Campaign program of the US Department of Energy (DOE), Office of Nuclear Energy. The report was authored by UT-Battelle under Contract No. DE-AC05-00OR22725 with the US DOE.

ABSTRACT

To support a multi-laboratory Methodology, Evaluation, Testing, and Analysis (M.E.T.A.) cladding properties database, Oak Ridge National Laboratory's (ORNL's) cladding mechanical test geometries were manufactured from several nuclear-relevant cladding alloys and subsequently tested. These geometries were developed as mechanical test specimens to evaluate the properties of tube materials that may be used for irradiation testing at ORNL's High Flux Isotope Reactor. They may also be used as test articles to be harvested—via in-cell machining—from commercially irradiated fuel rods and later tested. This report explores the differences among axial, hoop, and SSJ tensile geometries with partially recrystallized Zircaloy-2 to test ORNL correlation-based methods on a plate material that approximates, to the greatest extent possible, the characteristics of nuclear industry tubing. Furthermore, several tests were conducted with ORNL's Zircaloy-4 tube inventory to (1) develop material properties as a standard for future tests, (2) determine the effect of the US Department of Energy's Advanced Fuels Campaign coating processes on tube mechanical properties, and (3) evaluate the effect of specimen machining methods on the mechanical properties of tube geometries.

1. INTRODUCTION

1.1 AXIAL TENSION AND RING TENSION MECHANICAL PROPERTY CORRELATIONS

As the first barrier against nuclear fuel release, the mechanical integrity of nuclear cladding tubes is crucial for maintaining coolable geometries in a reactor and for avoiding rupture during long-term storage. Therefore, the mechanical properties of the tubes are important measures for quantifying manufacturing process quality, determining degradation effects from reactor environments, and evaluating safety margins for extended-life use or storage after they are removed from the reactor. Many methods exist for measuring the mechanical performance of nuclear tubes, such as ring compression testing [1, 2, 3, 4, 5], burst testing [4, 6, 7, 8, 9, 10], tube bending [11], and so on. Unfortunately, many of these methods test the tubing as a complicated structure, making mechanical property information difficult to obtain through strain gradients or complex loading paths [2, 4]; require precise measurement techniques that are difficult to implement in hot cell environments [6, 8]; or consume large amounts of valuable irradiated material [8, 11]. As a result, when characterizing the mechanical properties of a tube component, many researchers have machined tensile gauges in the axial or hoop directions [12, 13, 14, 15, 16] to perform a more conventional mechanical test to obtain the mechanical properties of the tube in its principal coordinates.

Although these specimen geometries can be leveraged to load the specimens primarily in the axial or hoop directions, the ring-type tensile geometries present many challenges that contaminate the mechanical properties that may be obtained. For instance, depending on the orientation of the ring tensile gauge relative to the loading mandrel, strain gradients may arise across the wall thickness or gauge length due to bending stresses or plastic hinge formation [17, 12, 18]. In some configurations, plastic hinges and bending stresses can saturate once the tensile specimen straightens, which leads to a complex load path on the specimen that is difficult to remove its bias on mechanical test data, especially in a hot cell environment. Furthermore, because the mandrels are loaded along the inside surface of the specimen, frictional forces bias the stress measurements to higher values, and specimens with longer gauge lengths often produce necks at two locations [13, 16], making it difficult to relate measured elongation from a mechanical test to real specimen elongation. To overcome these challenges, Oak Ridge National Laboratory developed millimeter-scale axial tension test (ATT) and ring tension test (RTT) specimens that minimize strain gradients across the specimen gauge [18] and consume less material than previous test methods did. Moreover, using an empirical strategy that correlates mechanical test specimen

engineering properties to more conventional tensile geometries, the mechanical properties in the hoop and axial directions can be measured in the hot cell.

Despite the successes of the mechanical test methodology, some challenges remain in establishing the testing techniques for wider use. For instance, the data used to correlate mechanical properties between specimen types in Gussev et al. [16] were taken from iron- or aluminum-based alloys that are dissimilar to the anisotropic, textured zirconium-based alloys used in the nuclear industry—except for one Zircadyne material tested. To further focus the approach employed by Gussev et al. on nuclear materials, work documented in this FY report included the testing of recrystallized, rolled Zircaloy-4 plate, which is a closer analog to industry nuclear claddings, to add that material to the current dataset. Moreover, the new shorter gauge length RTT specimen was developed in the time after that paper's release. Therefore, data that correlate the properties obtained with this new geometry were collected to supplement the previous datasets that quantify geometry-related effects on engineering mechanical properties.

1.2 AXIAL TENSION AND RING TENSION MECHANICAL PROPERTY DATABASE

The US Department of Energy's Advanced Fuels Campaign (AFC) is pursuing accident-tolerant fuel materials to increase the "coping time" in the event of a loss-of-coolant accident scenario [19, 20]. One of the main materials pursued by industry and the AFC is chromium-coated zirconium alloys because of their increased oxidation resistance. To facilitate these new materials' penetration into industry, they must first be shown to improve or do no harm in other aspects of nuclear safety. As a result, the mechanical properties of the as-received (AR) and coated materials must be obtained and understood to determine the effect of the coatings on the mechanical performance of the tubes. Furthermore, once these tests have been completed, the results of the mechanical tests must be organized and accessible to other researchers so that mechanical property information can be traced to causal manufacturing as well as environmental or test setup parameters. To that end, ATTs and RTTs were performed with AFC Zircaloy-4 and cold-spray and HiPIMS chromium-coated cladding tubes to determine the effect of the various coating methods on mechanical performance. Furthermore, these results are being uploaded to the AFC Materials Database, a database system in which test mechanical properties and metadata—such as test date, temperature, manufacturing information, specimen type, and so on—can be accessed by present and future users.

2. MATERIALS AND TESTING

ATT and RTT specimen geometries, as shown in Figure 1a and Figure 1b, respectively, were machined from fully recrystallized Zircaloy-2 plate from American Elements, with their tensile directions in the transverse and rolling directions. This tensile machining scheme is shown in Figure 2. Based on machine shop needs and costs, the tubes and specimen geometries were machined from the 1 cm thick plate via electrical discharge machining (EDM), except for the RTT specimens, which were EDMed to ring axial length, and the tensile gauge was end-milled. Tests were performed at room temperature and at 300°C on an Instron 5966 electromechanical test system with a strain rate of ~$1E^{-3}$ s^{-1}. RTTs were performed with the gauge in the 12 o'clock position along the mandrel, as shown in Figure 1c. Boron nitride was sprayed on the mandrel to reduce friction between the mandrel and the RTT specimens.

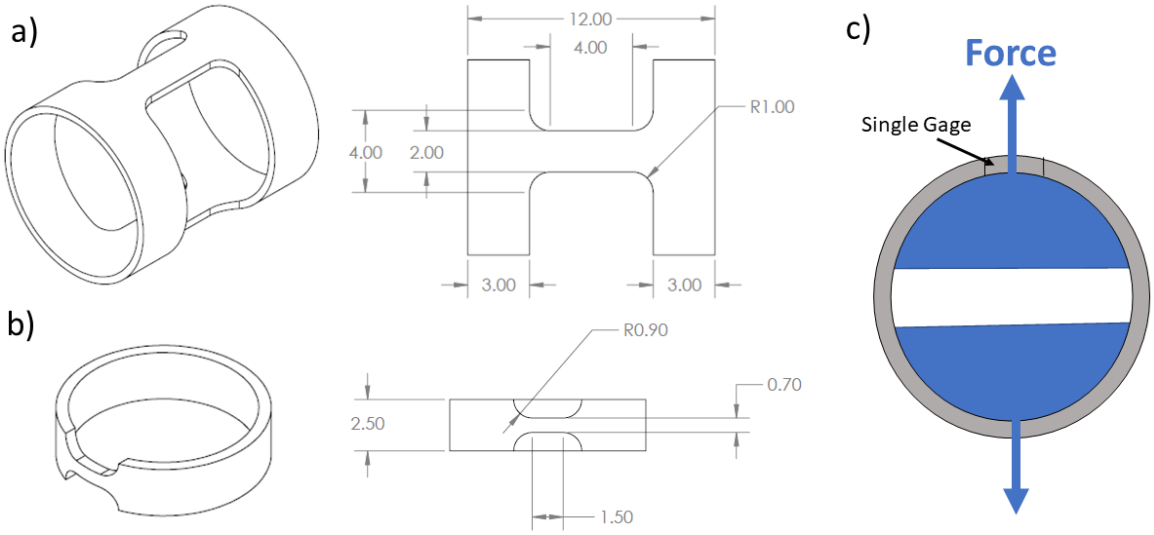

Figure 1. Specimen drawings of a) the ATT specimen and b) RTT specimen used in this work with c) a schematic showing the load configuration of the fixture used to load RTT specimens.

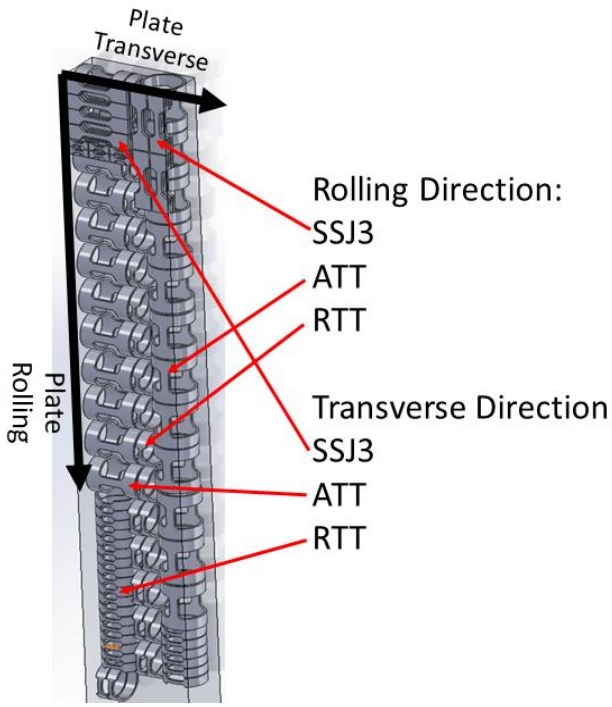

Figure 2. Machining schema for the ATT, RTT, and SSJ3 specimens that were manufactured out of Zircaloy-4 plate.

ATT and RTT specimens were also machined from ORNL's Zircaloy-4 cladding tube inventory and from cold-sprayed and HiPIMS-coated Zircaloy-4 tubing via EDM and via a computer numerical control (CNC) machine with a carbide end mill. This setup was used to obtain the coating materials' mechanical property information and to compare the sensitivities of the machining method used to manufacture the specimens. The Zircaloy-4 material was found to have divots on the outside surface that hindered coating adherence [20], so the Zircaloy-4 was hand-polished prior to coating. As a result, select tests were also performed with hand-polished uncoated tubes as well. More information on the Zircaloy-4 material can be found in Garrison et al. [21], and the coating methodologies can be found in Graening et al. [20]. Tests were performed at room temperature and at 300°C on an Instron 5966 electromechanical test system or on an MTS electromechanical system, based on system availability. Strain rates were kept the same as the zirconium plate tests' strain rate.

Digital image correlation was used to measure surface strains on select ATT and RTT specimens. Because the ring gauge was oriented toward the top of the mandrel, a prism was used, acting as a mirror so that the camera could capture the projection of the gauge surface. When DIC was implemented for RTTs, the inside surface of the specimens was sprayed with Boron nitride lubrication instead of spraying the mandrel; this was done to avoid spraying the prism with the lubricant.

The linear portion of the mechanical test curves depends on fixture compliance, machine compliance, and in the case of ATT specimens, the setting of the shoulders due to the shoulder loading configuration. To account for this variance in the linear portion of the mechanical tests, careful calibration would be required for all machines used for testing, or the crosshead displacement should be replaced by direct strain measurement using an extensometer. Unfortunately, these careful calibration procedures cannot be maintained in the hot cell, nor can the limited-dexterity hot cell manipulators reliably apply extensometers, especially to millimeter-scale mechanical test specimens. Moreover, requiring these calibration procedures to compare data collected across institutions would be costly. Because of this system-to-system sensitivity, the linear portions of the curves were removed from the data, so that plastic strain could be calculated from the crosshead displacement. As a result, all strains in this work are reported as plastic strains, which should be a more reproducible strain measurement between out-of-hot-cell and in-hot-cell systems—and these findings should also be directly comparable to results measured at other institutions for the same material.

3. RESULTS AND DISCUSSION

3.1 ZIRCALOY-4 PLATE TESTING

Mechanical tests with the fully recrystallized Zircaloy-2 plate were performed to obtain correlation factors for the shorter gauge length RTT specimen using a procedure similar to that used in Gussev et al. [16] to determine any anisotropy sensitivity to the correlation factors and to investigate potential temperature sensitivity to the correlation factors. Mechanical test results of the ATT, SSJ3, and RTT specimens are shown in Figure 3. Overall, the scatter in the ATTs and RTTs was larger than expected compared to that of industry-grade tubes. This result was attributed primarily to the machining method used. Specifically, tubes were EDMed from the plate material, then the ATT tensile gauges were EDMed and the RTT tensile gauges were end-milled. As a result, the EDM-affected layer is expected to be similar across all the specimens because the inside surface and outside surface of the 0.55 mm wall thickness tubes were EDMed; thus, machining effects on the mechanical property comparisons between specimen geometries from the plate are not expected to be significant. This is not a standardized, well-iterated procedure, so tube specimen quality suffered somewhat as could be compared to tubes manufactured via conventional means (pilgering, ball milling, etc.). Regardless, multiple specimens of the same processing direction and specimen type were tested, so the averages can be used to determine and evaluate correlation factors.

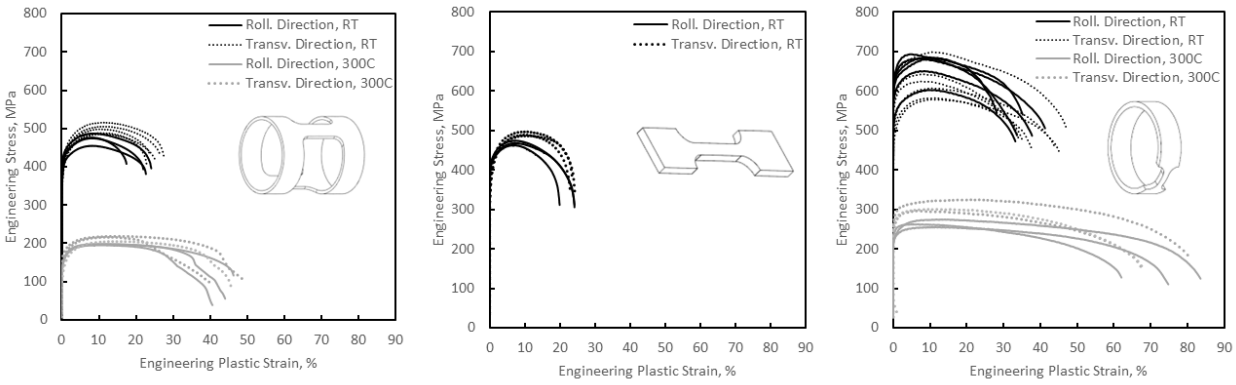

Figure 3. Mechanical test results of the fully recrystallized Zircaloy-4 plate. Specimen geometry is included in each plot.

The average and standard deviation of the engineering yield stress (YS), engineering uniform elongation (UE), engineering ultimate tensile strength (UTS), and engineering total elongation (TE) obtained from the tests are shown in Table 1 and Figure 4. It was found that the trends between rolling and transverse tensile specimen directions were preserved across specimen geometries, except for the UTS in the RTT configuration at room temperature and the TE in the RTT configuration at high temperature. This result suggests that these tube geometries do not exhibit significant sensitivity to anisotropy for these geometries. Furthermore, it was found that the data scatter in the properties obtained from the RTT configuration was larger than that of the ATT or SSJ configurations, which is consistent with previous observations [18]. This can partially be attributed to the tube machining method used via concentricity differences between the tube specimens and the mandrel, uneven lubrication application, differences in friction across the surfaces, or interactions associated with the smaller geometry limiting deformation [22]. However, it should be noted that in the case of deformation-limiting geometry, an ideal gauge geometry may not exist because the length and load configuration of the real tube component is limited by the tube circumference already. Mechanical tests with SSJ3 specimens at 300°C will be performed in the future.

Table 1. Engineering mechanical properties obtained from Zircaloy-4 plate.

				Average				Standard Dev.			
		Test. Temp.	# of tests	YS	UE	UTS	TE	YS	UE	UTS	TE
Direction	Specimen	ºC	#	MPa	%	MPa	%	MPa	%	MPa	%
Rolling	ATT	RT	4	402.8	8.24	478.7	21.56	8.4	0.29	5.0	2.50
	SSJ3	RT	3	402.5	7.29	468.8	22.76	2.4	0.27	4.8	1.99
	RTT	RT	6	592.1	8.79	666.7	34.86	35.2	2.60	31.4	4.06
Transverse	ATT	RT	5	382.9	11.00	507.6	25.29	15.9	0.12	19.0	1.68
	SSJ3	RT	3	353.8	10.18	491.3	23.59	6.1	0.63	4.4	0.58
	RTT	RT	6	535.7	9.98	622.7	40.51	50.2	1.52	40.9	5.09
Rolling	ATT	300	3	141.3	11.27	197.3	37.93	3.3	1.00	1.7	6.22
	RTT	300	3	223.9	10.83	264.5	72.60	7.3	4.27	8.0	9.02
Transverse	ATT	300	3	142.0	14.13	213.3	45.33	19.8	1.19	6.0	3.76
	RTT	300	3	260.6	13.77	307.8	72.23	10.0	6.33	12.5	6.06

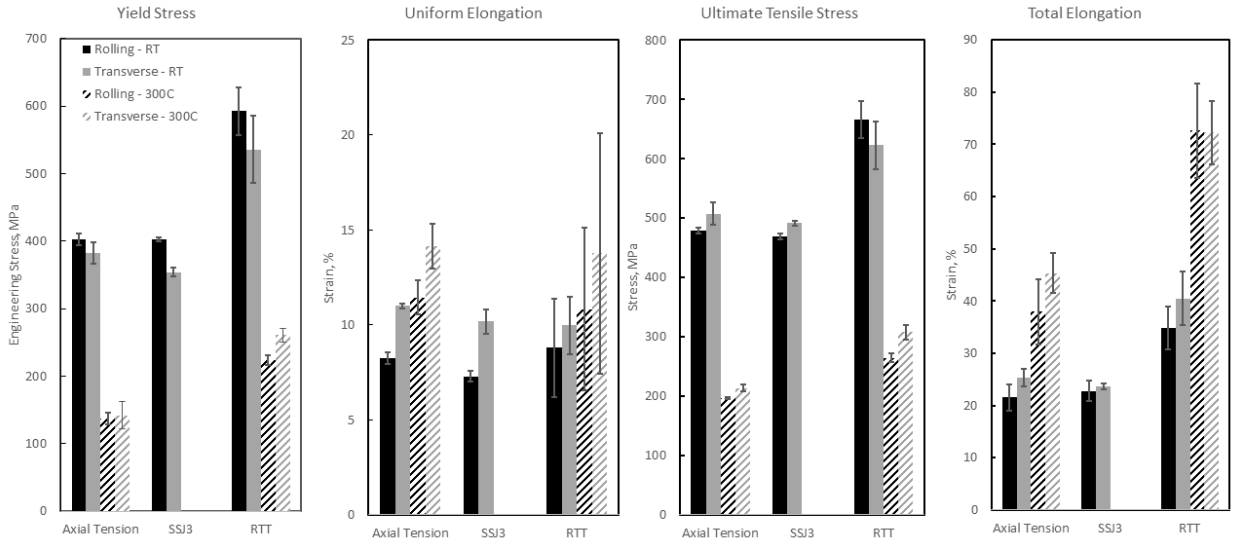

Figure 4. Engineering mechanical properties obtained for the fully recrystallized Zircaloy-4 plate showing that trends among the tensile geometries and cutting directions are maintained.

The stress-based correlation properties from ATT to SSJ3 in this work as compared to those reported in Gussev et al. [16] are shown in Figure 5a, and the strain-based properties are shown in Figure 5b. For UTS, UE, and TE, the new properties from both rolling and transverse direction tube specimens fell directly on the property curves, and for YS, both specimen machining directions fell acceptably close, suggesting that the anisotropic nature of the Zircaloy plate does not affect its correlations. High temperature results will be added to the correlations when the high temperature SSJ3 tests are completed.

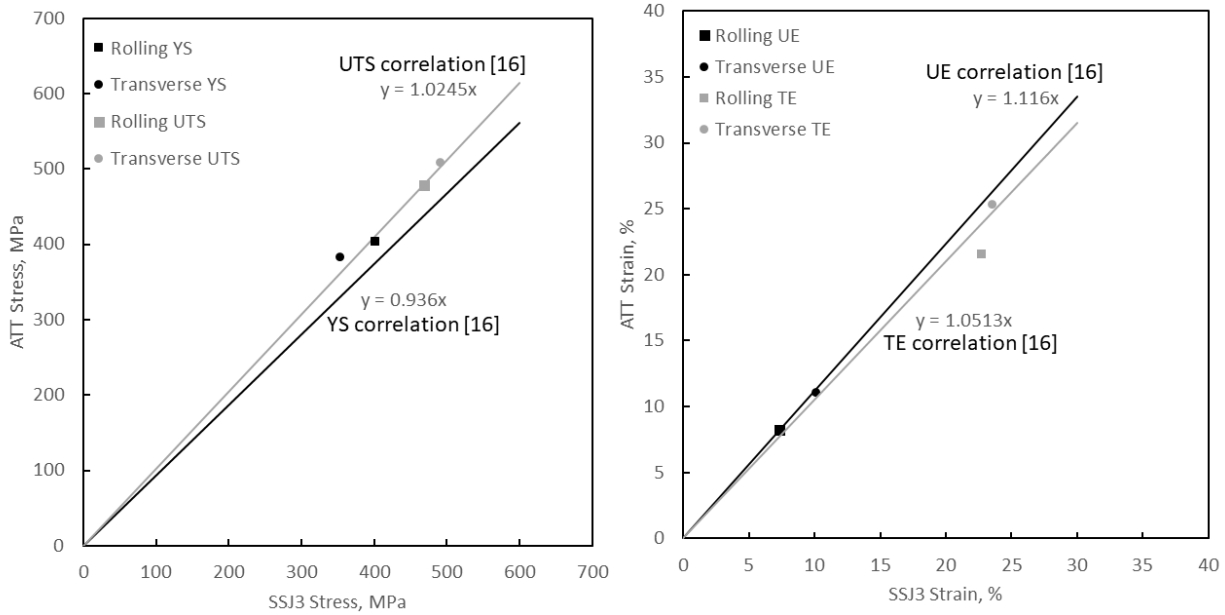

Figure 5. Correlation plots comparing the a) stress-based and b) strain-based engineering properties obtained from ATT specimens vs. those obtained from SSJ3 specimens tested under the same conditions. All tests were performed at RT.

RTT correlations are evaluated by correlations to properties obtained from ATT specimen geometry because of the lack of SSJ3 test data at high temperatures. Because Gussev et al. [16] used 3 mm and 7 mm gauge length RTT specimens and the specimens in this work had 1.5 mm gauge length, no direct comparison can be made to the data in the aforementioned work [16]. As a result, the correlations from the RTT tests were evaluated (1) as a trend from 7 mm length to 3 mm length to 1.5 mm gauge length and (2) based on the scatter associated with the current data line. The RTT correlations are shown in Figure 6. Results showed a clear trend in which the correlation value to ATT geometry increased for all properties as the gauge length decreased. For the stress-based values, this finding was the expectation: the part of the gauge that is necking and deforming was along the 12 o'clock portion of the mandrel, where friction was at its maximum. Similarly, for strain values, the correlation values also increased, which was expected from DIC analyses that showed that the longer gauge length specimens exhibited heavily localized deformation in the gauge length long before the ultimate tensile stress was reached. Importantly, the DIC analyses showed that an optical extensometer in the gauge length of the 1.5 mm gauge length specimen correlated 1:1 with the experimental curve from the test, which is consistent with the UE correlation value found to also be near 1 among the effective four materials tested. However, it was interesting to observe that the total elongation appears to be drastically over-estimated in the 1.5 mm gauge length specimens, suggesting that the small gauge may inhibit failure based on its effect of the changing stress state after necking occurs [22]. These correlations indicated no temperature dependence on the material correlations, but obtaining more data with the new RTT geometry is recommended.

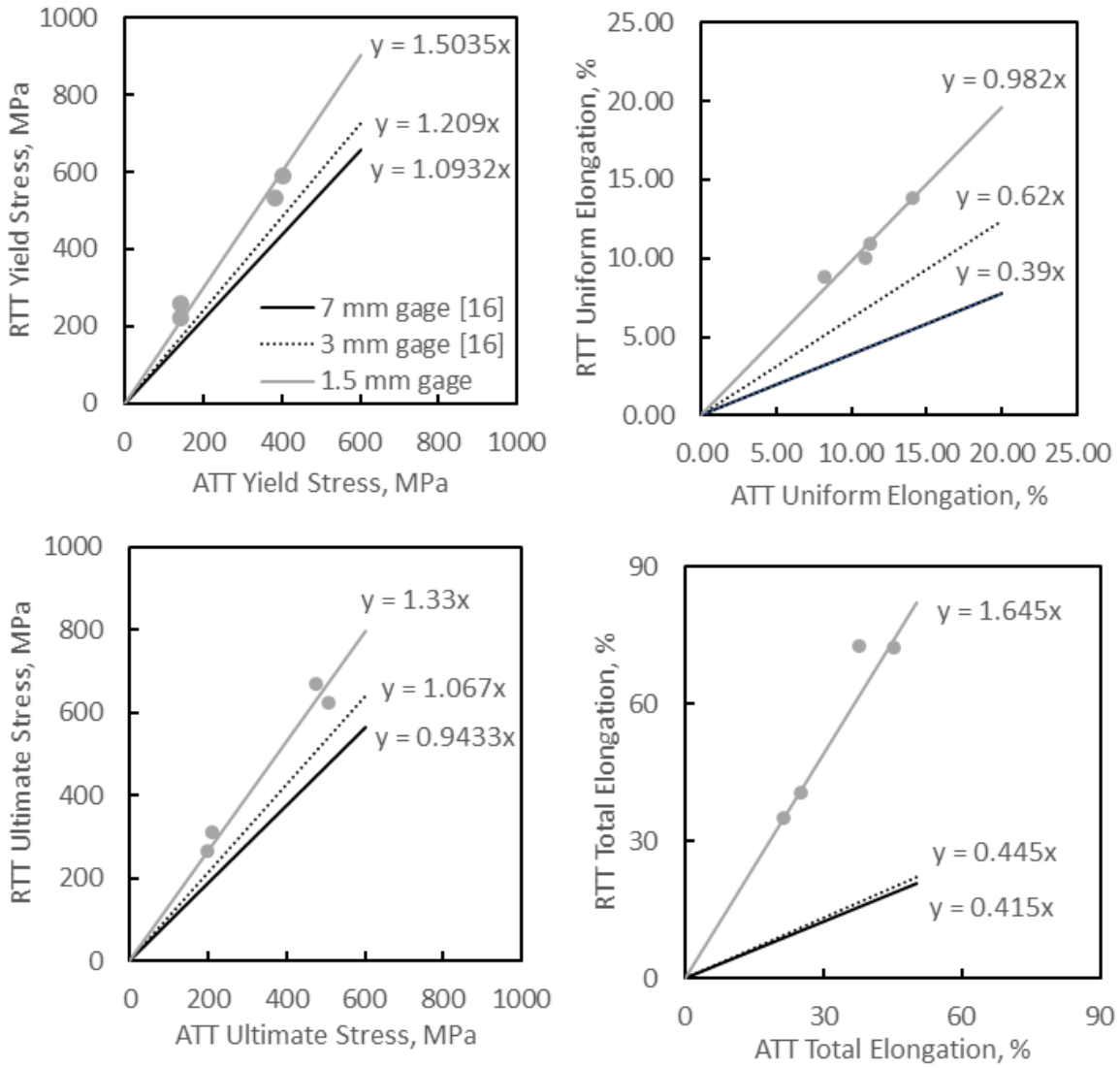

Figure 6. Engineering property correlations between RTT specimens and ATT specimens tested at the same conditions. The 3 mm gage length had a 0.8 mm gage width, and the 7 mm gage length had a 1.2 mm gage width.

3.2 ZIRCALOY-4 AND COATING IMPACT ON MECHANICAL PROPERTIES

ATT and RTT tests were performed with ORNL's AR Zircaloy-4 tubing as a benchmark and with several coated materials to evaluate the impact of the coating processes on the mechanical properties. ATT specimens were machined via EDM or CNC end milling to determine whether the machining method affected the mechanical properties. Mechanical test data are shown in Figure 7a for ATT tests at RT and 7b for ATT tests at 300°C, and the mechanical properties obtained from all the ATT tests are shown in Table 2. The plots show a clear trend in which the −100 V bias coated tubing showed increased strength in the axial direction relative to the AR tubing at the cost of a slight reduction in uniform and total elongation—but, importantly, the tubing retained significant ductility. The cold spray tubing showed a clear increase in strength and loss of uniform and total elongation in the axial direction at 300°C relative to the AR tubing but did not show a strength benefit at RT. The −150 V bias and −200 V bias showed a subtle strength loss and elongation increase relative to the AR tubing at both temperatures. It is important to note that the tubes were hand-polished prior to coating to improve coating adherence; thus, tests were also performed with hand-polished uncoated tubing to isolate the effect of the coating. It was clear that

the hand polishing had a minor effect on reducing the UE and UTS in the axial direction as the UE was ~3 standard deviations below the average UE for the end-milled AR tubing, and the UTS was ~1.5 standard deviations below the average UTS for the end milled tubing, but more testing is recommended.

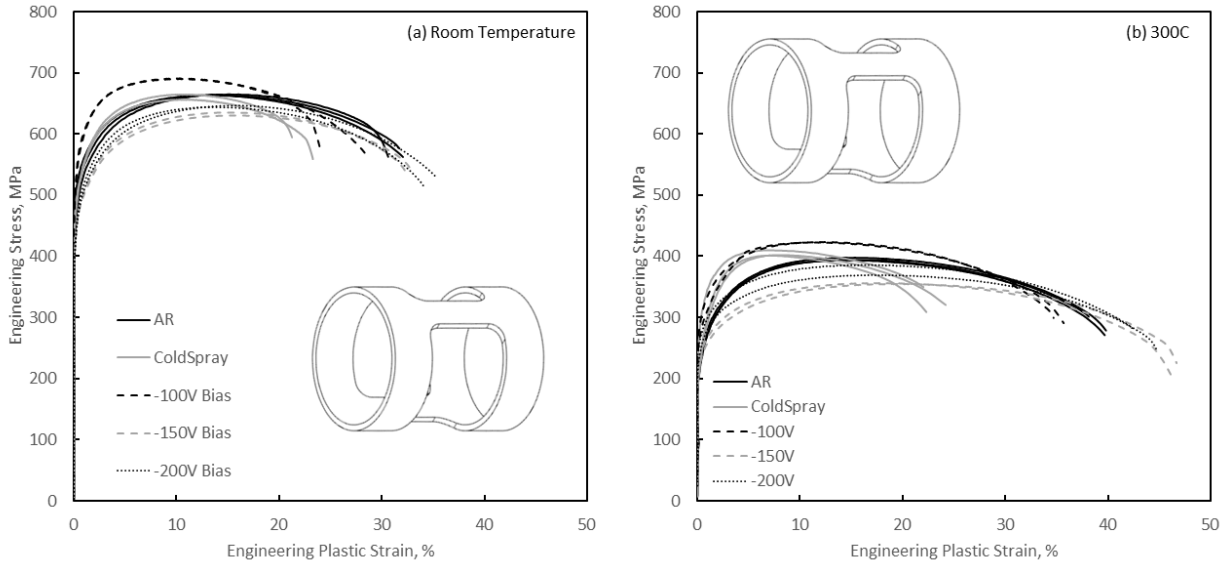

Figure 7. Mechanical test results a) at RT and b) at 300°C for ATT specimens machined from AFC Zircaloy-4 tubing and coated tubing. The tensile gauges for all specimens were EDMed.

Table 2. Mechanical properties obtained from ATT tests machined from AR and coated AFC-Zircaloy-4 tubing.

			number	Average Property				Standard Dev.			
Temp.			of tests	YS	UE	UTS	TE	YS	UE	UTS	TE
C	Material	Machining	#	MPa	%	MPa	%	MPa	%	MPa	%
RT	AR	EDM	6	492.1	13.57	662.2	31.88	13.2	0.53	7.6	0.52
		End Mill	1	469.8	11.10	628.5	28.40	—	—	—	—
	AR-Polish	End Mill	1	470.3	9.80	619.1	25.90	—	—	—	—
	ColdSpray	EDM	2	539.0	10.73	744.8	22.24	10.3	0.17	4.7	0.94
		End Mill	1	462.3	9.39	591.6	18.10	—	—	—	—
	−100V	EDM	2	520.9	9.80	690.7	26.30	1.8	0.00	0.4	2.40
		End Mill	1	490.7	9.90	605.1	24.60	—	—	—	—
	−150V	EDM	2	437.2	14.85	632.8	32.60	0.8	0.35	2.4	0.10
		End Mill	1	395.1	12.40	557.7	29.40	—	—	—	—
	−200V	EDM	2	435.4	14.75	645.2	34.70	3.4	1.35	1.3	0.70
		End Mill	1	422.9	11.60	564.2	30.60	—	—	—	—
300°C	AR	EDM	6	236.9	13.79	379.4	37.67	23.3	2.43	29.2	2.22
	ColdSpray	EDM	3	236.5	7.38	404.4	22.83	25.1	0.32	3.9	0.97
	−100V	EDM	3	286.3	11.80	417.5	35.64	19.1	0.12	8.0	0.76
	−150V	EDM	3	234.2	18.38	355.9	46.32	31.9	1.11	0.7	0.12
	−200V	EDM	3	244.7	16.72	380.4	43.66	9.7	0.51	7.8	0.95

ATT tests with end-milled specimens were tested to compare the effect of the machining method on the mechanical response of the specimens. These tests are shown in Figure 8. A large discrepancy was observed between end-milled and EDMed ATT specimens: almost every property was ≥ 2 standard deviations lower than its-end milled counterpart except for the UE and TE for the −100 V bias specimens. The trend among the coated specimens remained whether the specimens were EDMed or end milled: the −100 V bias was the strongest, followed by the cold spray, −200 V bias, and −150 V bias, but in end-milled specimens, the −100 V bias specimen exhibited a lower YS and UTS than the AR specimen, which deviated from the EDMed data. This could suggest that end milling removed some of the residual stresses expected from the coatings or that the coated materials are more affected by EDM. Regardless, more research is necessary to form a proper conclusion about why the coated material seems to be more strongly affected by machining method.

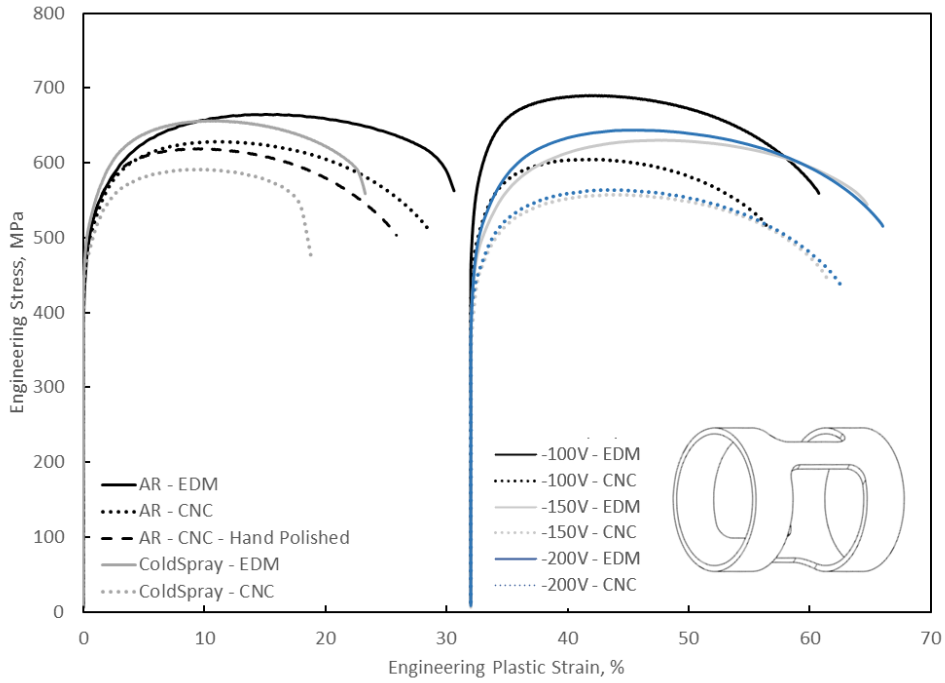

Figure 8. Mechanical tests with ATT specimens at RT showing the difference between the mechanical response of EDMed specimens vs. those end-milled on a CNC. −100 V bias, −150 V bias, and −200 V bias materials are shifted for chart clarity.

Mechanical test data for RTTs at RT are shown in Figure 9a, and RTTs for 300°C are shown in Figure 9b, and the mechanical properties obtained for the specimens are shown in Table 3. For RTT specimens, all the tensile gauges were machined via end milling. For reader clarity, not all specimens are included in the plots. All the coated specimens showed statistically equivalent or worse mechanical strength and ductility at RT and 300°C compared to the AR material in the hoop direction from RTT tests. This is the opposite expectation from improved burst test data and the expected residual compressive stresses [10] from the coating processes. The gap between the coated materials vs. uncoated specimens was observed to close as temperature increases, so more testing at higher temperatures may indicate improved performance at temperatures above 300°C where burst occurred. Otherwise, some of the gains in strength for the coated materials may come from residual compressive stresses in the axial direction that reinforce the tube as it is loaded biaxially from internal pressure, although hoop direction properties would be expected to dominate.

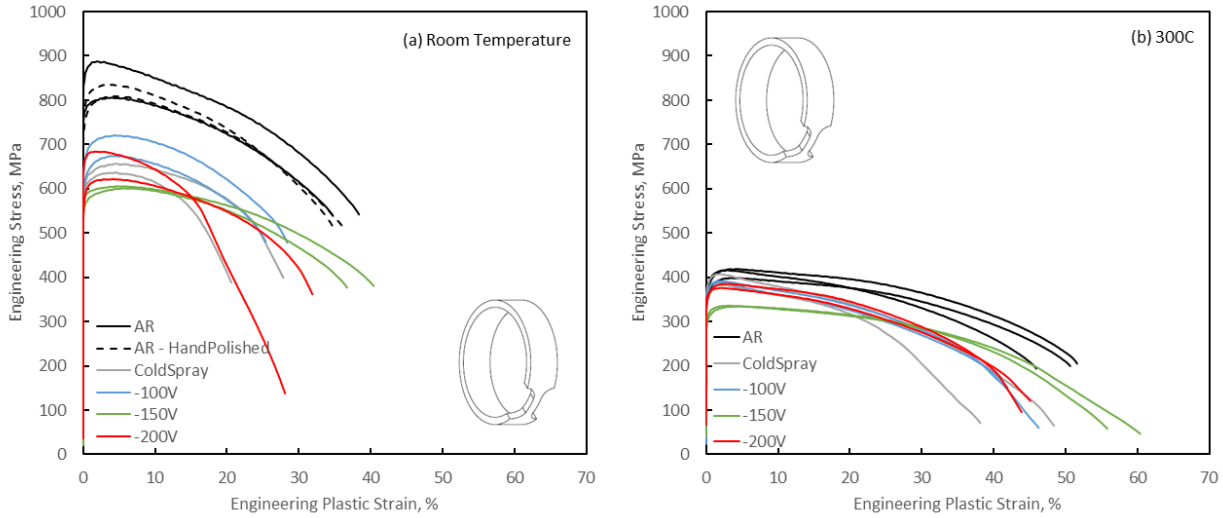

Figure 9. Mechanical test results a) at RT and b) at 300°C for RTT specimens machined from AFC Zircaloy-4 tubing and coated tubing. Results are not correlated to ATT or SSJ3 geometries, so friction has not been removed.

Table 3. Engineering mechanical properties obtained from RTT specimens machined from AFC Zircaloy-4 tubing tested at RT and 300°C. The tensile gauges for RTT specimens were all end-milled. Values here are uncorrelated to ATT or SSJ3 geometries.

Temperature		Number of tests	Average property				Standard Dev.			
			YS	UE	UTS	TE	YS	UE	UTS	TE
C	Material	#	MPa	%	MPa	%	MPa	%	MPa	%
RT	AR	5	773.2	4.89	818.2	36.74	22.6	0.79	22.7	1.82
	AR-HandPolish	2	761.0	4.20	822.4	35.50	18.3	0.20	13.0	0.70
	ColdSpray	2	597.1	4.55	646.9	24.20	5.2	0.05	9.8	3.60
	−100V	3	638.3	4.72	699.1	28.08	18.2	0.54	19.2	2.07
	−150V	2	568.3	5.20	603.7	38.55	10.7	0.50	2.4	1.85
	−200V	2	617.8	2.95	653.2	30.00	41.7	1.25	31.1	1.90
300°C	AR	3	365.4	3.66	411.6	49.37	9.2	0.55	9.0	2.48
	ColdSpray	2	363.5	1.83	395.3	43.25	15.9	0.01	12.0	5.12
	−100V	2	367.0	1.88	389.8	44.08	2.7	0.09	1.9	2.16
	−150V	2	306.7	3.93	335.6	58.07	4.8	0.78	0.7	2.28
	−200V	2	354.2	2.39	380.7	44.48	4.6	0.32	4.7	0.62

4. MATERIALS DATABASE

Following the testing of nuclear cladding materials, the specimen information and corresponding mechanical test data are being uploaded to a web-based relational database system [23, 24, 25]. This database system has benefited from over a decade of steady improvements in the Gen IV Materials Handbook Knowledgebase and the ASME Materials Properties Database: the system has been used to successfully maintain and manage data from multiple industries and countries [23, 24, 25].

The data record labeled *0023C_TENTest_Zircaloy-4-100V_AFC_ORNL_Y23M03D08_1* shown in Figure 10 was collected in FY23 from the −100 V bias coated AFC Zircaloy-4. Project information, specimen traceability information, tensile geometry measurements, tensile machining information, specimen drawings, and DIC information can be stored in the specimen information section. Similarly, a pre-test specimen conditioning section (not depicted) allows for storage of additional heat treatments, coating methods, surface preparations, or other parameters that can be added when needed. Furthermore, test parameters such as strain rates, test temperatures, and fixturing can also be added and customized for datasets that have specific measurements or parameters. The engineering properties measured from each test can be added for each specimen; the functional data (e.g., DIC images, DIC analysis data, stress vs. strain data or other test data) can also be added to each applicable specimen. Importantly, with all the data stored in the database, specimens can be selected at will, and the mechanical property data can be formulated into a table, as shown in Figure 11, or functional data can be plotted together.

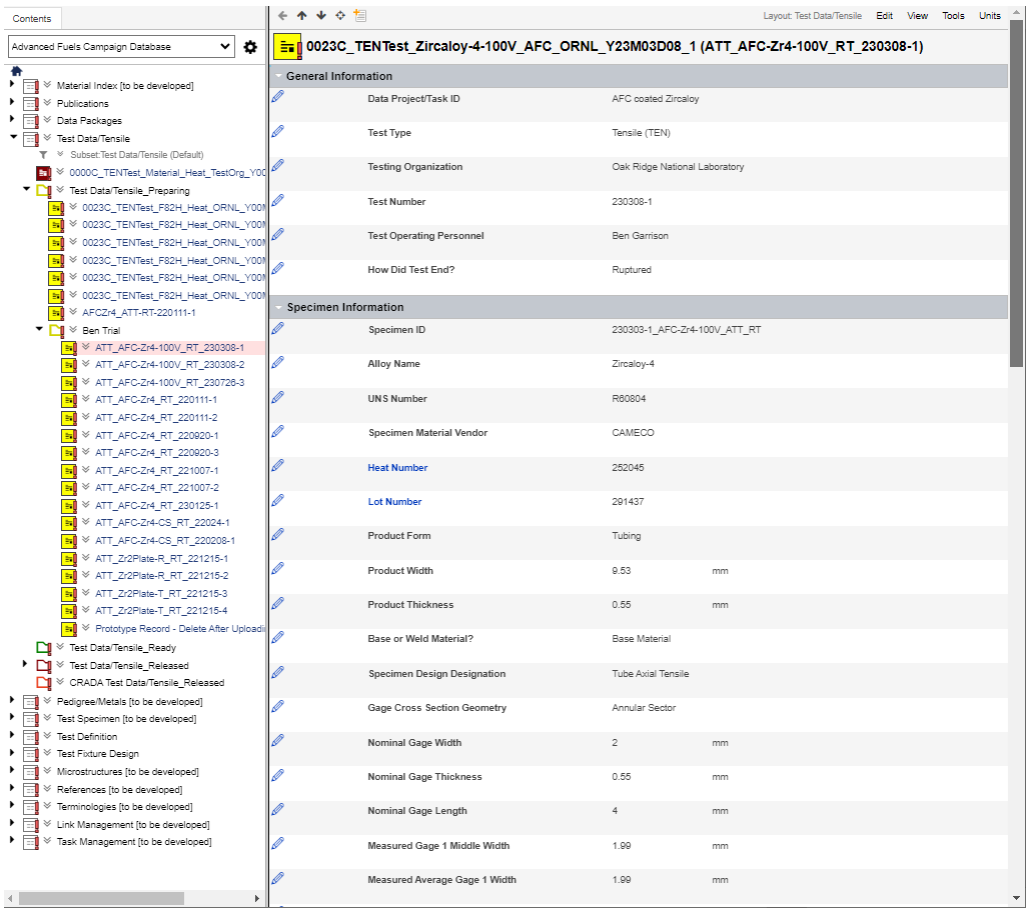

Figure 10. Image of the database interface showing how various specimen and material inputs can be tracked and accessed.

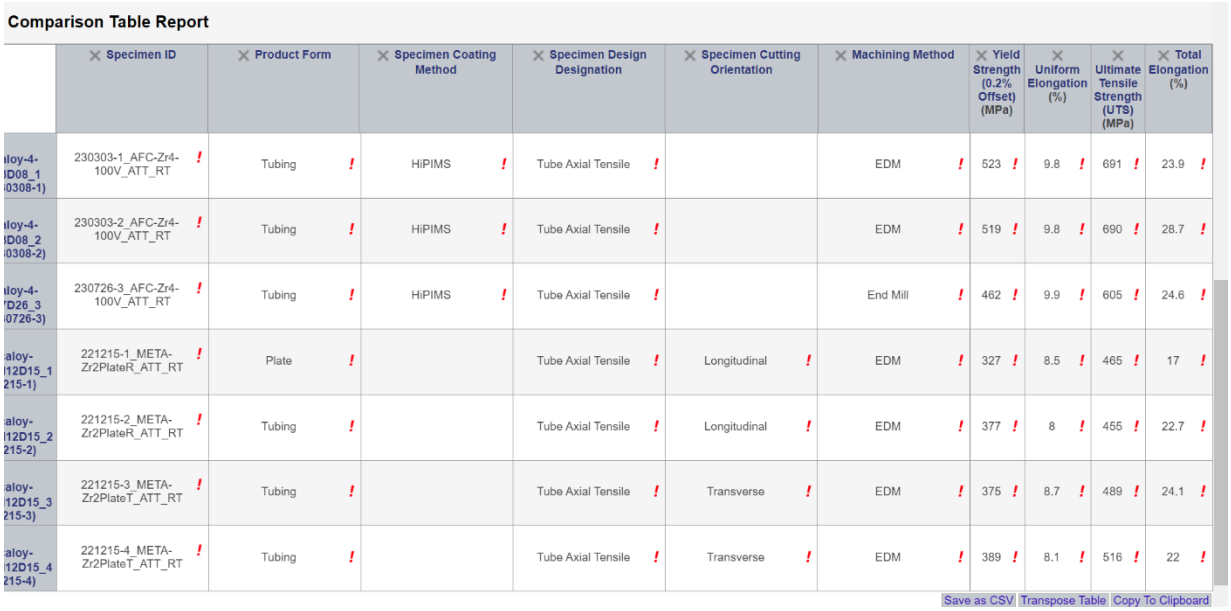

Comparison Table Report

	Specimen ID	Product Form	Specimen Coating Method	Specimen Design Designation	Specimen Cutting Orientation	Machining Method	Yield Strength (0.2% Offset) (MPa)	Uniform Elongation (%)	Ultimate Tensile Strength (UTS) (MPa)	Total Elongation (%)
loy-4-D08_1 0308-1)	230303-1_AFC-Zr4-100V_ATT_RT	Tubing	HiPIMS	Tube Axial Tensile		EDM	523	9.8	691	23.9
loy-4-D08_2 0308-2)	230303-2_AFC-Zr4-100V_ATT_RT	Tubing	HiPIMS	Tube Axial Tensile		EDM	519	9.8	690	28.7
loy-4-D26_3 0726-3)	230726-3_AFC-Zr4-100V_ATT_RT	Tubing	HiPIMS	Tube Axial Tensile		End Mill	462	9.9	605	24.6
aloy-12D15_1 215-1)	221215-1_META-Zr2PlateR_ATT_RT	Plate		Tube Axial Tensile	Longitudinal	EDM	327	8.5	465	17
aloy-12D15_2 215-2)	221215-2_META-Zr2PlateR_ATT_RT	Tubing		Tube Axial Tensile	Longitudinal	EDM	377	8	455	22.7
aloy-12D15_3 215-3)	221215-3_META-Zr2PlateT_ATT_RT	Tubing		Tube Axial Tensile	Transverse	EDM	375	8.7	489	24.1
aloy-12D15_4 215-4)	221215-4_META-Zr2PlateT_ATT_RT	Tubing		Tube Axial Tensile	Transverse	EDM	389	8.1	516	22

Save as CSV | Transpose Table | Copy To Clipboard

Figure 11. Example image of a table output from the database showing the engineering properties that can be accessed as well as functional data such as the stress strain curves (not depicted).

5. CONCLUSIONS

In this work, ATT and RTT mechanical tests were performed for the META and AFC programs. This testing leveraged short-length specimens that can be used to test cladding mechanical properties in the axial and hoop direction from tube specimens, both of which can be performed in a hot cell. ATT and RTT specimens were machined from rolled, fully recrystallized Zircaloy-4 plate that closely modeled that of cladding tube textures. The ATT specimens directly supplemented previous data from the literature [16], and correlation plots for shorter-gauge length RTT specimens were generated for a nuclear-relevant material. Moreover, the RTT correlation for UE was found to correlate nearly 1:1 with ATT specimens, which is consistent with previous DIC results that showed strain measurements correlating 1:1 with engineering plastic strain measurements.

Several ATT and RTT mechanical tests were performed with AR Zircaloy-4 tubing to produce statistically significant data for each specimen type. Furthermore, several coated Zircaloy-4 materials were tested and compared to the AR material, and some strengthening in the axial direction was found to have occurred from cold spray and −100 V bias materials, but a loss in mechanical strength was shown in the hoop direction from RTT tests. This result supports AFC's objective to evaluate the impact that Cr-coating procedures can have on the uncoated tubing's mechanical performance.

End-milled ATT specimens were directly compared to EDMed tubes of the same material, and it was found that end-milled mechanical properties deviated significantly from those obtained from EDMed specimens. EDM is expected to affect the specimen microstructure, thereby impacting the mechanical performance, so end milling machining procedures are recommended in the future. Finally, mechanical test data are being added to an online database for all the relevant data for each material and specimen type; this database system organizes the data obtained for the program so that several users can access and use it. This data acts as a benchmark and would directly support future research with more tubing materials including hydrided, oxidized and/or irradiated material in understanding the effect of the subsized specimens on the measured mechanical properties of HFIR-irradiated or commercially-irradiated materials.

6. REFERENCES

[1] M. A. Martin-Rengel, F. J. Gómez-Sánchez, J. Ruiz-Hervías and L. Caballero, "Determination of the hoop fracture propertie of unirradiated hydrogen-charged nuclear fuel cladding from ring compression tests," *J. of Nucl. Mat.,* vol. 436, pp. 123-129, 2013.

[2] B. Garrison, Y. Yan and S. TerMaath, "Determining failure properties of as-recieved and hydrided unirradiated Zircaloy-4 from ring compression tests," *Eng. Fail. Analysis,* vol. 125, p. 105362, 2021.

[3] J. Kim, M. Lee, B. Choi and Y. Jeong, "Effects of oxide and hydrogen on the circumferential mechanical properties of zircaloy-4 cladding," *Nuc. Eng. and Des.,* vol. 236, pp. 1867-1873, 2006.

[4] J. Desquines, D. Koss, A. Motta, B. Cazalis and M. Petit, "The issue of stress state during mechanical tests to assess cladding performance during a reactivity insertion accident (RIA)," *Journal of Nuclear Materials,* vol. 412, pp. 250-267, 2011.

[5] M. C. Billone, T. Burtseva and R. Einziger, "Ductile-to-brittle transition temperature for high-burnup cladding alloys exposed to simulated dyring-storage conditions," *J. of Nuc. Mat.,* vol. 433, pp. 431-448, 2013.

[6] N. Brown, B. Garrison, R. Lowden, M. Cinbiz and K. Linton, "Mechanical failure of fresh nuclear grade iron-chromium-aluminum (FeCrAl) cladding under simulated hot zero power reactivity initiatedaccident conditions," *Journal of Nuclear Materials,* vol. 539, 2020.

[7] B. Garrison, M. N. Cinbiz, M. Gussev and K. Linton, "Burst characteristics of advanced accident-tolerant FeCrAl cladding under temperature transient testing," *J. of Nucl. Mat.,* vol. 560, p. 153488, 2022.

[8] K. Kane, S. Bell, B. Garrison, M. Ridley, M. Gussev, K. Linton and N. Capps, "Quantifyin gdeformation during Zry-4 burst testing: a comparison of BISON and a combined in-situ digital image correlation and infrared thermography method," *J. of Nuc. Mat.,* vol. 572, p. 154063, 2022.

[9] S. Bell, K. Kane, C. Massey, L. Baldesberger, D. Lutz and B. Pint, "Strength and rupture geometry of un-irradiated C26M FeCrAl under LOCA burst testing conditions," *J. of Nuc. Mat.,* vol. 557, p. 153242, 2021.

[10] M. Ridley, S. Bell, B. Garrison, T. Graening, N. Capps, Y. Su, P. Mouche, B. Johnston and K. Kane, "Effects of Cr/Zircaloy-4 coating qualities for enhanced accident tolerant fuel cladding," *Ann. of Nuc. En.,* vol. 188, p. 109799, 2023.

[11] T. Narukawa and M. Amaya, "Four-point-bend tests on high-burnup advanced fuel cladding tubes after exposure to simulated LOCA conditions," *J. of Nuc. Sci. and Tech.,* vol. 57, pp. 782-791, 2020.

[12] F. Nagase, T. Sugiyama and T. Fuketa, "Optimized ring tensile test method and hydrogen effect on mechanical properties of Zircaloy cladding in hoop direction," *J. Nucl. Sci. and Tech.,* vol. 46, no. 6, pp. 545-552, 2009.

[13] M. K. Samal, K. S. Balakrishnan and S. Balakrishnan, "A practical approach to evaluate stress-strain behavior of remotely handled pressure tubes of nuclear reactors using ring tension test," *T. Indian I. Metals,* vol. 68, pp. 299-310, 2015.

[14] A. S. Frolov, I. V. Fedotov and B. A. Gurovich, "Evaluation of the true-strength characteristics for isotropic materials using ring tensile test," *Nuc. Eng. and Tech.,* vol. 53, no. 7, pp. 2323-2333, 2021.

[15] I. Barsoum and K. F. Al Ali, "A procedure to determine the tangiential true stress-strain behavior of pipes," *Int. J. Pres. Ves. Pip.,* vol. 128, pp. 59-68, 2015.

[16] M. N. Gussev, B. Garrison, C. P. Massey, A. Le Coq, K. Linton and K. A. Terrani, "A correlation-based approach for evaluating mechanical properties of nuclear fuel cladding tubes," *J. Nucl. Mat.*, 2022.

[17] C. P. Dick and Y. P. Korkolis, "Mechanics and full-field deformation study of the ring hoop tension test," *J. of solids and struc.*, vol. 51, no. 18, pp. 3042-3057, 2014.

[18] B. Garrison, C. P. Massey, M. Gussev, B. Sitterson, N. Capps and J. Harp, "Recent progress in mechanical testing of the nuclear fuel cladding materials," in *Structural Materials in Nuclear Science*, Idaho Falls, ID, 2022.

[19] K. Terrani, "Accident tolerant fuel cladding development: Promise, status, and challenges," *Journal o fNuclear Materials*, no. 501, pp. 13-30, 2018.

[20] T. Graening, B. Garrison, K. Kane, K. Linton and A. Nelson, "Impact of coating defects on performance of coated zirconium cladding," Oak Ridge National Laboratory, Oak Ridge, 2021.

[21] B. Garrison, K. Linton, K. K., S. Bell, S. Hawkins, B. Johnston, T. Graening and A. Nelson, "FY21 AFC burst activities with coated Zircaloy-4 under accident conditions," Oak Ridge National Laboratory, Oak Ridge, TN, 2021.

[22] O. N. Pierron, D. A. Koss and A. T. Motta, "Tensile specimen geometry and constitutive behavior of Zircaloy-4," *J. of Nuc. Mat.*, vol. 312, pp. 257-261, 2003.

[23] W. Ren, "Development of digital mateirals database for designe and construction of new power plants," in *Proceedings of 2008 International Congress on Advances in Nuclear Power Plants (ICAPP '08)*, Anaheim, CA, 2008.

[24] W. Ren, D. Cebon and S. Arnold, "Effective materials property information management for the 21st century," *J. of Press. Ves. Tech.*, vol. 133, no. 4, p. 044002, 2011.

[25] W. Ren, "Path forward: materials data modernization for ASME codes and standards in the artificial intelligence era," in *Proceedings of the ASME 2023 Pressure Vesssels & Piping Division Conference*, Atlanta, GA, 2023.